

## Suppressing large excursions to a chaotic attractor using occasional feedback control

P. Parmananda and M. Eiswirth

*Fritz-Haber-Institut der Max-Planck-Gesellschaft, Faradayweg 4-6, D-14195 Berlin, Germany*

(Received 17 November 1995; revised manuscript received 20 May 1996)

In certain nonlinear systems, under appropriate conditions, the dynamical behavior switches intermittently between two distinct chaotic states. We report the stabilization of the dynamics on a desired chaotic state using an occasional feedback control via a map-based algorithm which can be easily implemented in experimental situations where only one variable is observed. For the purpose of this paper implementation of the control strategy is restricted to systems characterized by one-dimensional next-amplitude maps. Possible applications are pointed out. [S1063-651X(96)51708-3]

PACS number(s): 05.45.+b

### I. INTRODUCTION

Since the advent of the OGY [1] control technique, chaotic behavior has been suppressed in various experimental situations [2–6]. These experiments use the original algorithm or its various modifications [1,7,8] to convert the observed chaotic behavior to periodic responses. However, recently some work has been done in chaos anticontrol [9–11]. This includes methods for sustaining chaos in systems exhibiting intermittent chaotic behavior where chaotic response is interrupted by periodic episodes. This recent emphasis on trying to maintain chaos is motivated by the fact that the destruction of chaotic behavior is undesirable in certain biological systems. Some recent studies suggest that pathological destruction of chaotic behavior could be an underlying reason for heart failures [12] and certain kinds of brain seizures [11].

In this paper we wish to extend the concept of maintaining chaos in dynamical systems that exhibit intermittency involving switching between two distinct chaotic states. In the context of this paper it implies that the chaotic attractor is a composite of two distinct pieces and the dynamics switch intermittently between these two pieces (states). Such dynamical behavior is associated with systems exhibiting deterministic crises.

Using a control strategy similar to the one proposed by In *et al.*, we were able to select and stabilize the dynamics of one of the two distinct pieces (corresponding to a particular state) using an occasional feedback control. The only previous effort involving similar control, that we are aware of, is the work done by Nagai and Lai [13]. They used a control strategy based on the technique of targeting [14], to select and stabilize a desirable chaotic state in the Ikeda map. However, in contrast to the present work, their strategy is difficult to implement [13] in real experimental situations.

Besides possible application to biological systems [13,15], the present method could find application in any of the various systems exhibiting deterministic crises [16–19]. In the following section we discuss the control strategy. In Sec. III, we present results from the implementation of the control algorithm to a numerical model for a chemical oscillator and the standard Lorenz model. Finally in Sec. IV we offer a brief conclusion.

### II. CONTROL STRATEGY

The control strategy used is similar to the one proposed by In *et al.* and relies only on experimentally measured quantities. We restrict ourselves to its one-dimensional implementation and hence the only prerequisites are the following:

(i) The dynamics of the system can be represented by a nonlinear map given by  $X_{n+1}=f(X_n,P)$ . In autonomous systems, such a map can be easily obtained, for example, by plotting successive extrema from the time series of the observable.

(ii) Small variations in the control parameter  $P$  about the setpoint  $P_0$  shift the position of the attractor but do not change the shape significantly.

(iii) Finally, there is at least one specific region of the map (termed the “transition region”) that lies on the attractor and which the system visits before executing the undesirable chaotic behavior.

Once the return map has been obtained from the time series, for example, by plotting successive extrema, the transition regions are determined by observing the iterates of the system as it approaches the undesirable chaotic behavior. The extent of each of these transition regions is determined by the distribution of points in that region. We then pick  $T_m$ , the transition region to implement control on, where  $T_m$  is the interval in the return map composed of the  $m$ th preiterates which occur before the undesirable chaotic state (large-amplitude oscillations) is visited.

Then following the OGY [1] strategy we move the attractor slightly by varying the control parameter  $P$  and observe the resulting change in the location of the next iterate which corresponds to the  $(m-1)$ th preiterate before an excursion (called  $T_{m-1}$ ). This allows us to calculate  $g$  defined as the shift of the transition region ( $T_{m-1}$ ) per unit change of the control parameter,

$$g = \frac{\delta f(X_n, P)}{\delta P}.$$

Now control is implemented when the system enters the predesignated transition region  $T_m$ . Since the location and the extent of the region  $T_{m-1}$  is known from previous observations, we can calculate  $d_{m-1}$  defined as the minimum dis-

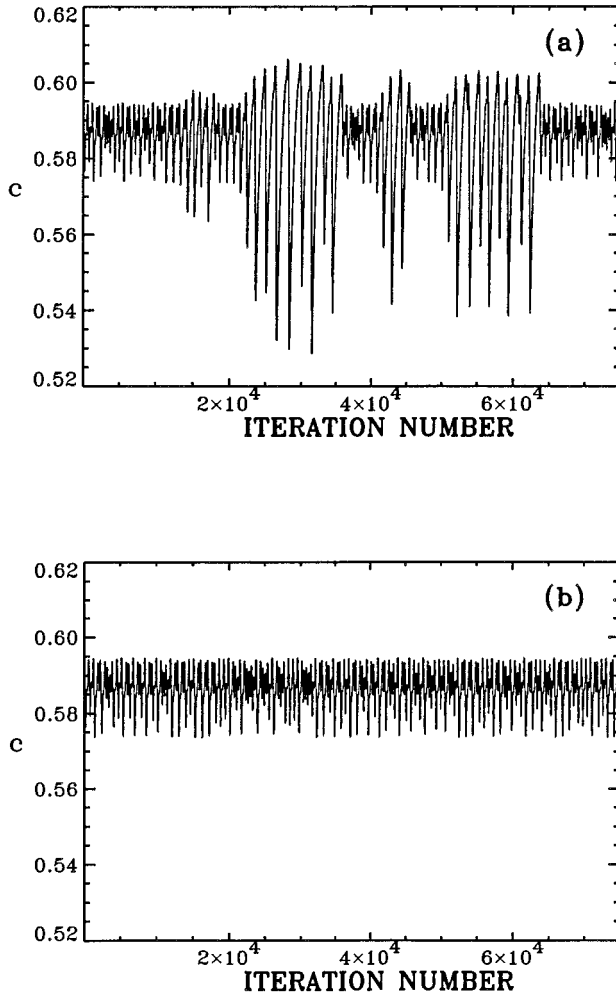


FIG. 1. (a) Uncontrolled time series of the state space variable  $c$  plotted for the numerical model of a chemical oscillator [Eq. (1)]. The value of the control parameter  $d=0.134$  is chosen so that the observed chaotic behavior is a composite of two states with distinct amplitudes. The  $\delta t$  chosen for integration was 0.1 in dimensionless units of time. (b) Controlled time series of the state space variable  $c$  plotted for the chemical oscillator. All large-amplitude oscillations are suppressed. The perturbations to the control parameter  $d$  to achieve and maintain control were less than 0.5% of  $d_0=0.134$ .

tance by which the attractor needs to be shifted such that the next iterate of the return map falls out of the extent of the region  $T_{m-1}$ . This distance ( $d_{m-1}$ ) is translated into a corresponding parameter change  $\delta P$  given by  $\delta P = d_{m-1}/g$ . Following In *et al.* [10], we initially circumscribed the transition interval  $T_{m-1}$  by a circle of radius  $r_{m-1}$  as the worst case scenario, hence recalculating the desired parameter change as

$$\delta P = 2r_{m-1}/g.$$

This change in parameter  $\delta P$  is an occasional feedback control allowing us to stabilize the desired chaotic state. The

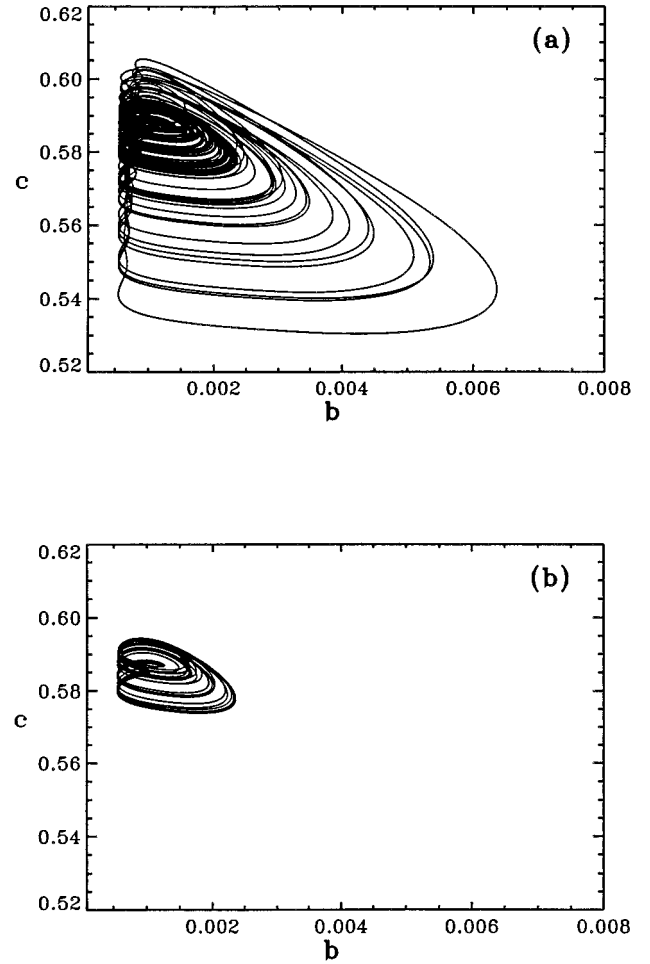


FIG. 2. (a) Two-dimensional projection of the uncontrolled chaotic attractor for the time series shown in Fig. 1(a). 75 000 iterates are plotted to obtain the attractor. (b) Two-dimensional projection of the controlled chaotic attractor for the time series shown in Fig. 1(b). 25 000 iterates are plotted to obtain the attractor.

parameter change can be subsequently reduced without any loss in efficiency by carefully examining the shape of the transition regions [10].

To summarize, a perturbation  $\delta P$  is added to the control parameter  $P$  each time an iterate of the map enters the transition region  $T_m$  such that the next iterate falls outside the transition region  $T_{m-1}$ . This avoids the occurrence of the undesirable chaotic state corresponding to large-amplitude oscillations.

### III. APPLICATION TO MODELS

We now apply the control strategy discussed in the preceding section to two model systems where the observed chaotic behavior is a composite of two distinct states. In both cases the fourth preiterate was chosen to implement control such that the third preiterate (and the subsequent undesirable behavior) was precluded.

The first system is the model for a chaotic chemical oscillator [20] described by the following set of differential equations [20]:

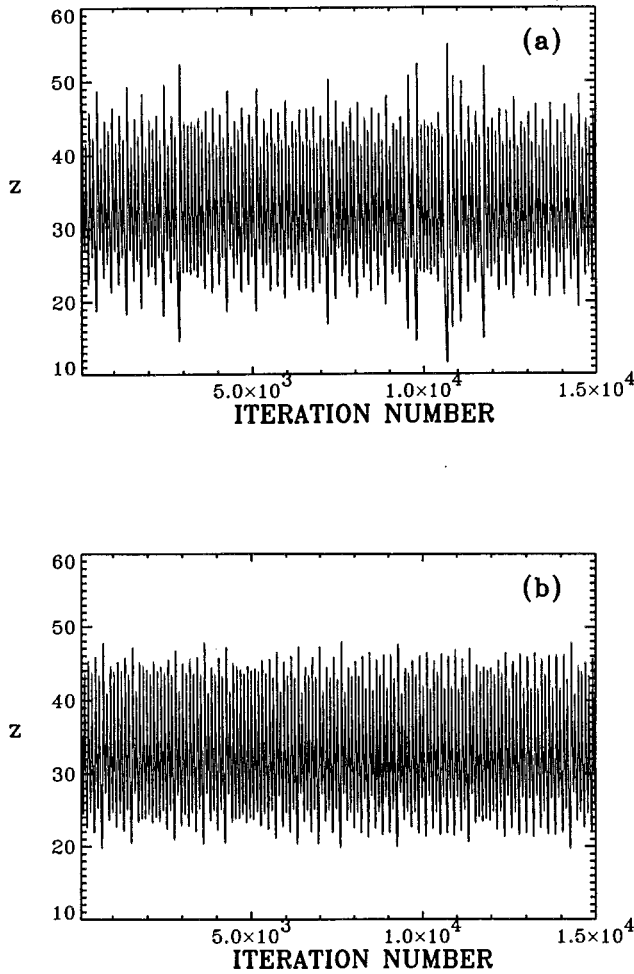


FIG. 3. (a) Uncontrolled time series of the state space variable  $z$  plotted for the Lorenz model. The system parameters are  $\sigma=12.1$ ,  $\rho=35.0$ , and  $\beta=1.0$ . The  $\delta t$  chosen for integration is 0.01 in dimensionless units of time. (b) Controlled time series for the Lorenz system. The time series is devoid of large-amplitude oscillation ( $z \geq 48$ ). The corrections to the control parameter were about 1–2% of  $\sigma_0=12.1$ .

$$\begin{aligned} \dot{a} &= k_1 a c - k_2 a - k_3 a b / (a + K) + k_4 d, \\ \dot{b} &= k_2 a - k_5 b + k_6, \\ \dot{c} &= k_7 - k_1 a c - k_8 c, \end{aligned} \quad (1)$$

where  $a$ ,  $b$ , and  $c$  are the three independent variables and  $d$  is chosen to be the bifurcation parameter. For  $0.130 < d < 0.137$  the system is chaotic [20]. Upon decrease of  $d$ , the system undergoes an interior crisis at  $d = 0.13562$ , hence for  $d \geq 0.13562$  the amplitude of the chaotic behavior is small, whereas for smaller  $d$  small chaos is interrupted by episodes of large-amplitude oscillations. The values of the other parameters are chosen to be constant [20] at  $(k_1, k_2, k_3, K, k_4, k_5, k_6, k_7, k_8) = (2, 0.4, 1.0, 0.0001, 0.002, 0.5, 0.0002, 0.005, 0.0068)$ .

Figure 1(a) shows the time series of the state space variable  $c$  at  $d = 0.134$  ( $d$  was chosen to be the control parameter). The chaotic behavior observed is alternating between

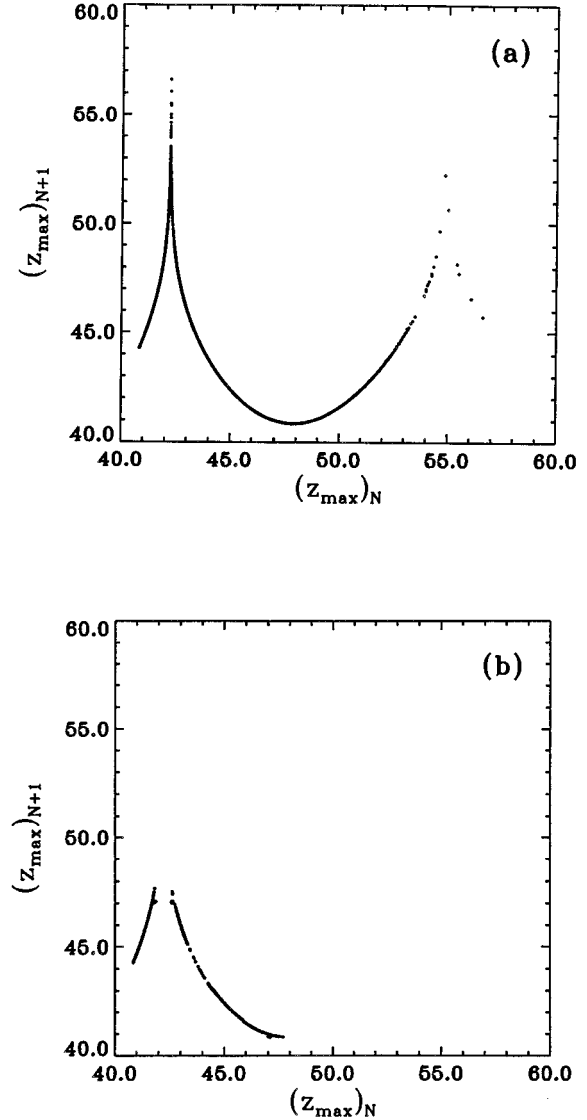


FIG. 4. (a) Return (next-maximum) map for the uncontrolled time series in Fig. 3(a). About 5000 maxima are used to obtain the return map. (b) Return map obtained using the time series in Fig. 3(b) while the control is being implemented (2000 maxima). The confinement of the size of the attractor in comparison to (a) is evident from the suppression of the second maximum in the return map showing that the dynamics is being controlled on the chaotic phase corresponding to the small-amplitude oscillations.

large- and small-amplitude oscillations. The corresponding two-dimensional projection of the chaotic attractor is shown in Fig. 2(a). The different probability of orbit visits for the two distinct parts of the chaotic attractor is manifested by the contrast in the point density. We implemented the occasional feedback strategy to try to eliminate the state corresponding to the large-amplitude oscillations in the following manner.

From the maxima of the time series shown in Fig. 1(a) we mapped out the transition region in the attractor which the system visits as a precursor to exhibiting large-amplitude oscillation. Then using the control strategy as discussed in the preceding section we observed the extent of these transition regions ( $T_m$ ) and their shift per unit change of the control parameter ( $d$ ). This enabled us to calculate the pertur-

bation ( $\delta d$ ) (added to  $d$ , once the system iterate enters a predesignated transition region  $T_m$ ) required to prevent the system from exhibiting the chaotic behavior corresponding to large-amplitude oscillations.

Figure 1(b) shows the time series for the model system while the control is being implemented. The system, by virtue of the control, is constrained to exhibiting small-amplitude oscillations. Figure 2(b) shows the corresponding attractor which exhibits the confinement of the system dynamics to a region of the phase space. The typical changes in the parameter value in order to achieve and subsequently maintain control were always less than 0.5% of  $d_0$  (typically  $\delta d = 0.0002$ ).

Next we report the application of the confinement to the Lorenz model:

$$\begin{aligned} \frac{dx}{dt} &= \sigma(y-x), \\ \frac{dy}{dt} &= x(\rho-z)-y, \\ \frac{dz}{dt} &= xy-\beta z. \end{aligned} \quad (2)$$

At low values of  $\beta$  ( $<0.7$ ) the system exhibits small-amplitude chaos with a single maximum in the return map [21,22], however, for  $\beta > 0.71$  the small oscillations are interrupted by a large excursion, occurring more and more frequently with increasing  $\beta$ . Here we choose  $[\sigma, \rho, \beta] = [12.1, 35.0, 1.0]$ . Figure 3(a) shows the autonomous chaotic times series. The large excursions ( $z > 48$ ) are suppressed by the control [Fig. 3(b)]. Here the effect of the control is most

clearly visible in the return map. Without the control the next-maximum map exhibits two maxima [Fig. 4(a)] the second of which is not visited any more after switching on the control [Fig. 4(b)], reflecting a confinement of the chaotic attractor. The regions corresponding to the excursion and the ensuing behavior are eliminated.

The control as discussed earlier was implemented by monitoring the location, extent and finally the shift of the transition ( $T_m$ ) regions.  $\sigma$  was chosen to be the control parameter and successive maxima in the state space variable  $z$  were used for analysis. As before, the control is implemented each time the trajectory entered a predetermined region of the attractor. Perturbations of the order of 1–2% (typically  $\delta\sigma = 0.01$ ) were required to achieve control.

#### IV. CONCLUSIONS

The control strategy presented does not require any knowledge of the underlying model. In fact, all the required information can readily be obtained from experimental measurement of a single observable. It should be possible to extend the strategy to systems with higher embedding dimensions. This would involve monitoring transition regions of higher dimensions. Control is therefore expected to be achievable in experimental situations whenever two distinct chaotic states occur, as is the case, for example, after occurrence of an interior crisis [23].

#### ACKNOWLEDGMENTS

We would like to thank G. Ertl for helpful discussions and R. W. Rollins of Ohio University for a critical reading of the manuscript. One of us (P. P.) acknowledges financial support from the Alexander von Humboldt foundation.

- 
- [1] E. Ott, C. Grebogi, and J. A. Yorke, *Phys. Rev. Lett.* **64**, 1196 (1990).
  - [2] W. L. Ditto, S. N. Rauseo, and M. L. Spano, *Phys. Rev. Lett.* **65**, 3211 (1990).
  - [3] E. R. Hunt, *Phys. Rev. Lett.* **67**, 1953 (1991).
  - [4] R. Roy, T. Murphy, Jr., T. D. Maier, Z. Gills, and E. R. Hunt, *Phys. Rev. Lett.* **68**, 1259 (1992).
  - [5] V. Petrov, V. Gáspár, J. Masere, and K. Showalter, *Nature* **361**, 240 (1993).
  - [6] P. Parmananda, P. Sherard, R. W. Rollins, and H. D. Dewald, *Phys. Rev. E* **47**, R3003 (1993).
  - [7] B. Peng, V. Petrov, and K. Showalter, *Physica A* **188**, 210 (1992).
  - [8] R. W. Rollins, P. Parmananda, and P. Sherard, *Phys. Rev. E* **47**, R780 (1993).
  - [9] W. Yang, M. Ding, A. Mandell, and E. Ott, *Phys. Rev. E* **51**, 102 (1995).
  - [10] V. In, S. E. Mahan, W. L. Ditto, and M. L. Spano, *Phys. Rev. Lett.* **74**, 4420 (1995).
  - [11] S. J. Schiff, K. Jerger, D. H. Duong, T. Chang, M. L. Spano, and W. L. Ditto, *Nature* **370**, 615 (1994).
  - [12] M. A. Woo, W. G. Stevenson, D. K. Moser, R. M. Haper, and R. Trelease, *Am. Heart J.* **123**, 704 (1992).
  - [13] Y. Nagai and Y. Lai, *Phys. Rev. E* **51**, 3842 (1995).
  - [14] T. Shinbrot, E. Ott, C. Grebogi, and J. A. Yorke, *Phys. Rev. Lett.* **65**, 3215 (1990).
  - [15] L. D. Iasemidis, J. C. Sackellares, H. P. Zaveri, and W. J. Williams, *Brain Topogr.* **2**, 187 (1990).
  - [16] C. Grebogi, E. Ott, and J. A. Yorke, *Physica D* **7**, 181 (1983).
  - [17] S. M. Hammel, C. K. R. T. Jones, and J. V. Moloney, *J. Opt. Soc. Am. B* **2**, 552 (1985).
  - [18] J. C. Sommerer, C. Grebogi, and E. Ott, *Phys. Rev. A* **43**, 1754 (1991).
  - [19] A. L. Goldberger, L. J. Findley, M. R. Blackburn, and A. J. Mandell, *Am. Heart J.* **107**, 612 (1984).
  - [20] J. L. Hudson, O. E. RöSSLer, and H. Killory, *Chem. Eng. Commun.* **46**, 159 (1986).
  - [21] E. N. Lorenz, *J. Atmos. Sci.* **20**, 130 (1963).
  - [22] J. M. T. Thompson and L. B. Stewart, *Nonlinear Dynamics and Chaos* (Wiley, New York, 1986).
  - [23] K. Krischer, M. Lübke, W. Wolf, M. Eiswirth, and G. Ertl, *Ber. Bunsenges. Phys. Chem.* **95**, 820 (1991).